

Electronic Supplementary Information

In-mold patterning and actionable axo-somatic compartmentalization for on-chip neuron culture

Ayako Yamada,[§] Maéva Vignes,[§] Cécile Bureau, Alexandre Mamane, Bastien Venzac, Stéphanie Descroix, Jean-Louis Viovy, Catherine Villard,* Jean-Michel Peyrin,* and Laurent Malaquin*

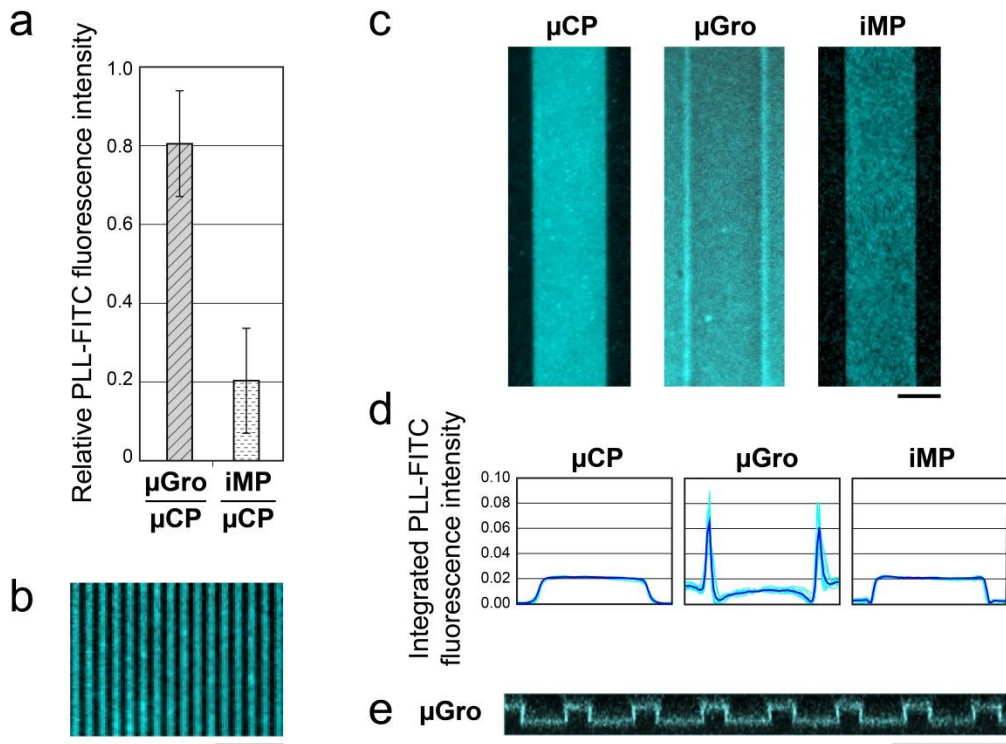


Figure S1. PLL coating properties on different substrates. (a) Relative fluorescence intensities of PLL-FITC on μGro and iMP substrates compared to μCP substrates. Values from at least 5 different areas in each experiment were averaged and compared between 4 sets of experiments. Error bars represent standard deviations. PLL-FITC densities on μCP and μGro substrates are comparable, whereas that on iMP is smaller than the others. (b) Fluorescence image of a PLL-FITC micro-pattern of 5 μm -wide tracks with 5 μm intervals on a μCP substrate. (c) Fluorescence images of PLL-FITC at the middle of 80 μm -wide tracks on different substrates. (d) Normalized profiles of the integrated PLL-FITC fluorescence intensity across the tracks. Thin (clear blue) lines in each graph represent the profiles of 10 different samples and the thick (dark blue) line represents their average. The origin of the peaks observed for μGro is explained in (e) showing a cross-sectional image of PLL-FITC fluorescence on μGro 20 μm -wide tracks obtained from a 12.6 μm -thick stack of confocal microscopy images. Scale bars, 50 μm .

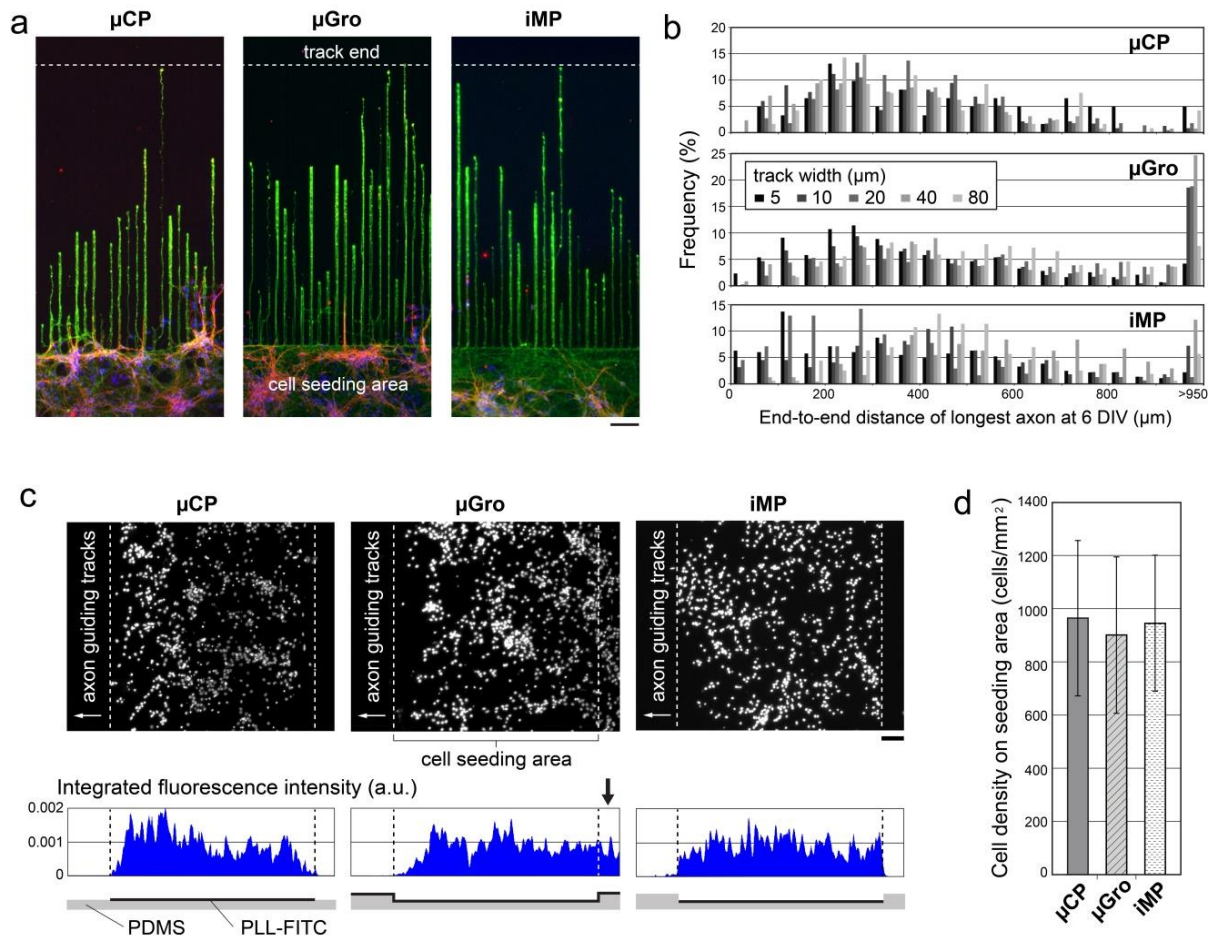


Figure S2. Axonal outgrowth and cell capture efficiency on different substrates. (a) Immunofluorescence images of neurons at 6 days in vitro (DIV) on different substrates with 10 μ m-wide guiding tracks with 20 μ m intervals. Axons (green), dendrites (red), and nuclei (blue) are stained by using anti-Tau, anti-MAP2 antibodies, and Hoechst, respectively. (b) Normalized histograms showing the distribution of the end-to-end distances between the tip of the longest axon and the entrance on each track at 6 DIV, with different track widths (w) for μ CP (top), μ Gro (middle), and iMP (bottom). The peaks at the highest value correspond to the highest extension corresponding to the full length of tracks. Globally, axons reach comparable lengths on the three different substrates and for different track widths. For $w = 5, 10, 20, 40, 80 \mu\text{m}$, the number of tracks (n) were: $n = 61, 233, 219, 128, 119$ (μ CP); $n = 429, 641, 776, 466, 305$ (μ Gro); and $n = 429, 641, 776, 466, 305$ (iMP), respectively, obtained from 2-5 different individual experiments. (c) Distribution of nuclei at 6 DIV on different substrates: fluorescence

microscopy images of nuclei stained with Hoechst (top), their integrated fluorescence profile (middle), and illustrated cross-sectional configurations of the substrates (bottom). On the μ Gro substrate, nuclei also adhere outside the cell seeding area, as indicated with a black arrow. (d) Cell densities on the seeding area on different substrates, measured on 10 samples for each substrate. Error bars represent standard deviations. Scale bars, 100 μ m.

Text S1. Additional text about axonal behavior within tracks

Besides the practical applications of iMP for axon guidance, from a fundamental point of view, our study shed light on the behavior of axons in different conditions of confinement. We observed an affinity of axons for edges, particularly pronounced on μ Gro in which axons can interact with the attractive PLL on two perpendicular faces. This behavior results in the formation, first of individual aligned axons, then of straight axonal bundles at latter stages. Axons on μ Gro tracks tend therefore to have more straight trajectories than those on μ CP or iMP substrates. This might help axons to reach a larger length, especially on wide tracks. Indeed, a slight difference in L in favour of μ Gro versus μ CP samples, which increases with track width, is observed (ESI Fig. S3). μ Gro also yielded the largest number of axons reaching the end of the track for large tracks (ESI Fig S2b). This alignment, however, is not associated with superior confinement into the tracks, as an axon aligned along a corner can escape with equal probability along the bottom surface or along the edge, since both are PLL-coated.

By contrast, axonal guidance by edges is regularly disrupted for iMP and μ CP by escapements (rebounds) from edges. This observation suggests different mechanisms of interaction between the growth cone and the border of the guiding track, depending on the nature of the substrates. In the case of purely chemical constraint, i.e. μ CP, axons with a high incident angle generally turn to become parallel to the track border, minimizing the angle from the original direction (ESI Fig. S4a). They tend to follow the edge for several tens of microns before deviating from the edge. Bouncing and consequent oscillations are seen rarely, and only in narrower tracks (ESI Fig. S4b). We expect that in such conditions, the absence of adhesive molecules prevents the thin and dynamic actin structures present at the front of the growth cone, the filopodia, to explore areas out of the track. The trajectory of the axons, which are guided by filopodia traction,¹ is thus deviated towards a direction closer to that of the border of the track. The fact that axons then continue along the track for a while, and do not often rebound, as could be expected due to the traction exerted by filipodia firmly attached on the surface of the track, is more surprising. This could be an effect of the accumulation of filipodia along the edge of the track, or to the rigidity of the axonal shaft (due to the bending rigidity of the microtubule axonal core). Whatever the physical origin of this phenomenon, it induces some

persistence of the growth direction before turning away from the border. Note that this persistency is also evidenced at the end of the μ Gro tracks. The same interpretation can apply to the case of iMP, in which the walls of the microstructures have no adhesive molecule, as shown by the similarity of the density profiles in Fig. 5c.

1. L. A. Lowery and D. Van Vactor, *Nat Rev Mol Cell Biol*, 2009, **10**, 332-343.

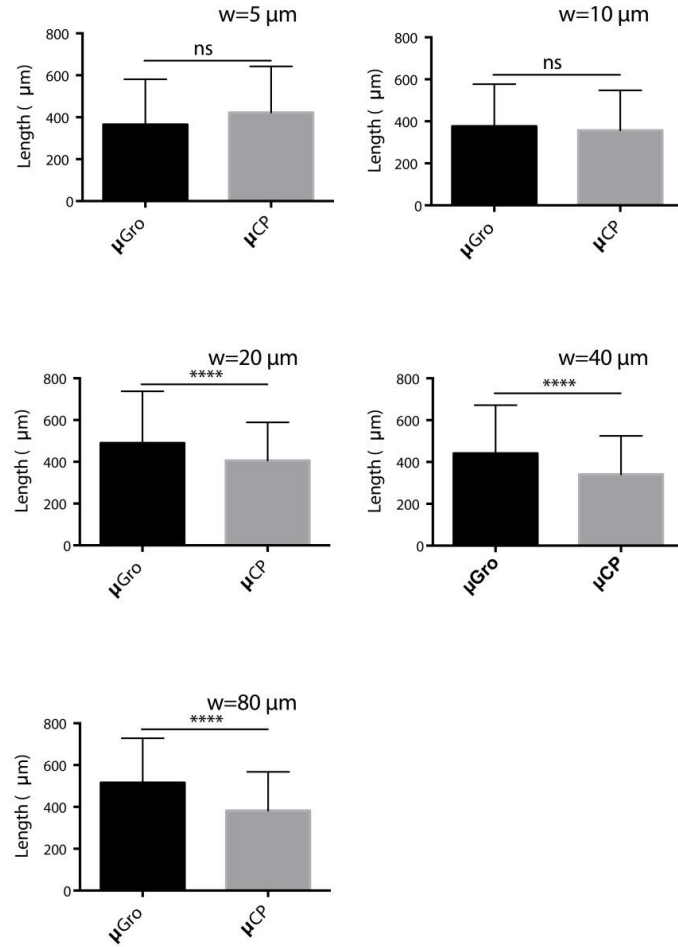


Figure S3. Axon length distributions for each track width for the two techniques sharing a similar PLL coating density, i.e. μGro and μCP. Bars represent the standard deviations. Mann-Whitney tests: $p = 0.0602$ ($w = 5 \mu\text{m}$, $n_{\mu\text{Gro}} = 411$, $n_{\mu\text{CP}} = 58$), $p = 0.2352$ ($w = 10 \mu\text{m}$, $n_{\mu\text{Gro}} = 522$, $n_{\mu\text{CP}} = 231$), $p < 0.0001$ ($w = 20 \mu\text{m}$, $n_{\mu\text{Gro}} = 630$, $n_{\mu\text{CP}} = 215$), $p < 0.0001$ ($w = 40 \mu\text{m}$, $n_{\mu\text{Gro}} = 351$, $n_{\mu\text{CP}} = 127$), $p < 0.0001$ ($w = 80 \mu\text{m}$, $n_{\mu\text{Gro}} = 282$, $n_{\mu\text{CP}} = 149$).

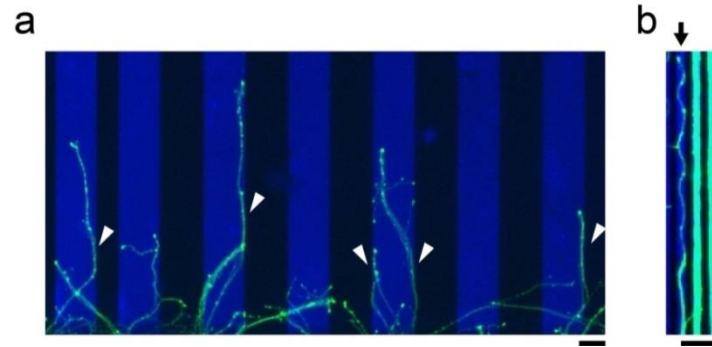


Figure S4. Fluorescence images of Tau-immunostaining (green) and PLL-FITC tracks (blue) on μ CP substrates. (a) After hitting against the border of the tracks, axons follow the border for a while before deviating from it (arrowheads). (b) In rare cases, seen on tracks with a width $w \leq 20$ μm , axons rebound after hitting the border (arrow). Scale bars, 50 μm .